Cooling of hot carriers in three- and two-dimensional $Ga_{0.47}In_{0.53}As$

H. Lobentanzer, W. Stolz, J. Nagle, and K. Ploog
Max-Planck-Institut für Festkörperforschung, Heisenbergstrasse 1, 7000 Stuttgart 80, Federal Republic of Germany
(Received 3 October 1988)

Carrier cooling is investigated by means of time-resolved photoluminescence spectroscopy in an undoped $Al_{0.48}In_{0.52}As/Ga_{0.47}In_{0.53}As/InP$ heterostructure and in undoped and modulation-doped $Ga_{0.47}In_{0.53}As/Al_{0.48}In_{0.52}As$ multiple-quantum-well structures. The cooling dynamics of electrons and holes is analyzed by a theoretical model based on Fermi-Dirac statistics and taking into account polar-optical scattering and acoustic-deformation-potential scattering as energy-loss and Auger processes as heating mechanisms. The energy loss of holes by polar-optical scattering is close to theoretical expectations in the low-excitation regime, but is reduced by 2 orders of magnitude for high-excitation densities. This reduction is attributed to a hot phonon effect. For electrons the polar-optical energy-loss rate is strongly reduced even at low excitation densities as compared to theoretical expectations. We assume that screening of the Coulomb interaction between carriers and lattice might play a role beside the hot phonon overpopulation to explain this phenomenon.

I. INTRODUCTION

The investigation of carrier-phonon interactions has been a topic of major importance in semiconductor research during the last years. Interest in these interactions is motivated by fundamental aspects as well as by their potential for device applications.

In the field of fundamental physics, research concentrates on the investigation of the strength of the different carrier-phonon interactions and the dependence on carrier density and dimensionality. Switching times of devices as well as materials degradation are strongly influenced by hot carrier effects. Therefore a systematic study of typical cooling times as well as of carrier-phonon interaction in specimens with different structural composition and by that way possibly enhanced or reduced energy-loss rates (ELR's) of hot carriers probably leads to faster devices or improved device lifetimes.

Previous experimental investigations on carrier-phonon interactions have been focused on the $Al_xGa_{1-x}As/GaAs$ system because of the favorable energy gaps and the well-developed crystal-growth technique. A comprehensive overview of the experimental and theoretical state of the art is given by Shah.[1]

The enormous technological importance of the ternary semiconductor $Ga_{0.47}In_{0.53}As$ requires an understanding of carrier-phonon interaction and of hot carrier effects in this material also. Carrier energy relaxation has been investigated by means of time-resolved photoluminescence by Kash and Shah[2] in a $Ga_{0.47}In_{0.53}As$ epilayer and with cw photoluminescence by Shum and co-workers.[3] In both papers a remarkably reduced polar-optical ELR was claimed, which was found to be independent of excitation density.

Recently, we carefully investigated the ELR of hot carriers in undoped bulk $Ga_{0.47}In_{0.53}As$ and undoped and n-type modulation-doped $Ga_{0.47}In_{0.53}As/Al_{0.48}In_{0.52}As$ multiple-quantum-well (MQW) structures in a cw experiment[4] and with time-resolved photoluminescence.[5–7] The following facts have been established by our work.

(i) For low excitation density the polar-optical ELR of carriers in undoped $Ga_{0.47}In_{0.53}As$ samples (bulk or MQW's) can be described satisfactorily by using the theoretical value of the Fröhlich coupling constant for the polar-optical energy loss. (ii) A reduction of the polar-optical ELR by 2 orders of magnitude is observed for high excitation densities. (iii) The polar-optical ELR of hot electrons in an n-type modulation-doped $Ga_{0.47}In_{0.53}As/Al_{0.48}In_{0.52}As$ MQW is reduced by a factor of 35 even for very low excitation density. (iv) Deformation-potential scattering and heating by Auger processes have to be included for the interpretation of cooling data in $Ga_{0.47}In_{0.53}As$. In the cited publications we have investigated undoped and n-type modulation-doped material; therefore a separation of the energy-loss rates of electrons and holes was impossible.

In the present paper we extend our experimental investigations in the following two directions.

(1) We perform a systematic study of the well-thickness dependence of the energy-loss rates of carriers in undoped $Ga_{0.47}In_{0.53}As/Al_{0.48}In_{0.52}As$ MQW's.

(2) We investigate n- and p-type modulation-doped $Ga_{0.47}In_{0.53}As/Al_{0.48}In_{0.52}$ MQW's. In that way we can separate, especially for polar-optical scattering, energy loss by electron–LO-phonon scattering and by hole–LO-phonon scattering, and study the excitation density dependence of each scattering mechanism nearly independently. Our new presented data enable us to give a consistent picture of carrier cooling and allow us to understand qualitatively the mechanisms, which reduce the polar-optical energy loss at high excitation densities.

The paper is organized as follows. In Sec. II, details of the experimental setup and the structural parameters of the samples are described. In Sec. III the cooling of hot carriers in a $Ga_{0.47}In_{0.53}As/Al_{0.48}In_{0.52}As/InP$ heterostructure is discussed in detail. A theoretical model is

presented, which uses Fermi-Dirac statistics for electrons and holes, and takes into account polar-optical scattering, acoustic deformation-potential scattering, and carrier heating by Auger processes. The data are analyzed with this theoretical model. In Sec. IV a systematic study of the well-thickness dependence of energy loss by polar-optical scattering, acoustic deformation-potential scattering, and Auger processes in undoped $Ga_{0.47}In_{0.53}As/Al_{0.48}In_{0.52}As$ MQW's of different well thickness is performed. In addition, the intersubband relaxation of electrons, which are excited into higher subbands by the laser pulse, is discussed. The influence of carriers generated by doping on the cooling process is investigated in Sec. V. Analyzing the cooling behavior in n and p-type modulation-doped MQW's, we can separate the energy loss by electron–LO-phonon scattering from that by hole–LO-phonon scattering. In particular, these two energy-loss rates show a completely different dependence on excitation density, which allows us to identify the underlying mechanisms for the observed reduction of the polar-optical energy loss at least for the p-type modulation-doped and the undoped samples. In Sec. VI an interpretation of the data and a consistent picture of polar-optical scattering is given. The presented results are finally compared with results published by other groups. The conclusions (Sec. VII) summarize the experimental data about the cooling of hot carriers in two- and three-dimensional $Ga_{0.47}In_{0.53}As$.

II. EXPERIMENT

The samples used for the experiment are grown by molecular-beam epitaxy (MBE) and lattice matched on (100) InP substrates.[8] The bulk sample consists of an unintentionally doped 0.75-μm-thick $Ga_{0.47}In_{0.53}As$ layer, which is clad by a 1.25-μm-thick $Al_{0.48}In_{0.52}As$ layer. The $Ga_{0.47}In_{0.53}As$ layer is thick enough to show no quantization of energy levels. On the other hand, effects of inhomogeneous excitation and therefore diffusion into the depth do not seriously affect the evaluation of the experimental data. The undoped MQW's are composed of 150 (70, 50) $Ga_{0.47}In_{0.53}As$ quantum wells (QW's) of 3.4 (8.0, 13.8) nm width alternating with unintentionally doped 11.4-nm-thick $Al_{0.48}In_{0.52}As$ barriers. The various well thicknesses allow a systematic study of the ELR of the carriers as a function of well width. The n-type modulation-doped MQW's consists of 50 unintentionally doped $Ga_{0.47}In_{0.53}As$ QW's of 3.4 (8.2) nm width alternating with 23-nm-thick $Al_{0.48}In_{0.52}As$ barriers. The barriers are composed of 8.5-nm-thick undoped spacer layers, which clad a doped center region of 6-nm thickness. The p-type modulation-doped sample is composed similarly. The carrier density per QW in the modulation-doped samples has been determined by Hall measurements as well as by Shubnikov–de Haas experiments and amounts to 4×10^{11} cm^{-2} for the n-type and 2×10^{11} cm^{-2} for the p-type modulation-doped sample. All sample parameters are compiled in Table I. A more detailed description is given by Stolz *et al.*[8,9] The experimental setup for time-resolved photoluminescence is shown schematically in Fig. 1. The samples (sample temperature 5 K) are excited by a synchronously pumped mode-locked dye laser with a repetition rate of 80 MHz and a pulse duration of 4 ps. The dye laser is operated at a wavelength of 840 nm using the dye Styril 9. The photons with an energy of 1.48 eV are therefore absorbed only in the $Ga_{0.47}In_{0.53}As$ layers. The maximum average power is 50 mW, which is attenuated with neutral density filters as well as by varying the size of the laser focus. The size of the focus is measured carefully with calibrated pinholes. By these procedures we can vary our excitation density between 2×10^{18} and 5×10^{16} cm^{-3} in the case of the bulk sample and the corresponding two-dimensional (2D) densities for the MQW's. The photoluminescence is spectrally dispersed by a 0.32-m monochromator and temporally resolved by a 2D Hamamatsu synchroscan streak camera with an S1 cathode. The energy resolution of this set up amounts to approximately 3 meV and the time resolution is limited to 15 ps due to temporal broadening by the spectrometer and the trigger jitter of the streak camera. In our experiment we are able to measure simultaneously the luminescence as a function of time and of wavelength. The sensitivity of the whole system is carefully gauged with a calibrated tungsten lamp. After correcting for the spectral sensitivity, we can evaluate transient luminescence spectra and the luminescence lifetimes of our samples.

TABLE I. Structural parameters of the samples.

Sample	Well thickness L_z (nm)	Barrier thickness L_B (nm)	Type	Doping density (cm^{-2})
A	bulk			
B	3.4	11.4	undoped	
C	8.0	11.4	undoped	
D	13.8	11.4	undoped	
E	3.4	23	n	4×10^{11}
F	8.2	23.2	n	4×10^{11}
G	8.1	24.3	p	2×10^{11}

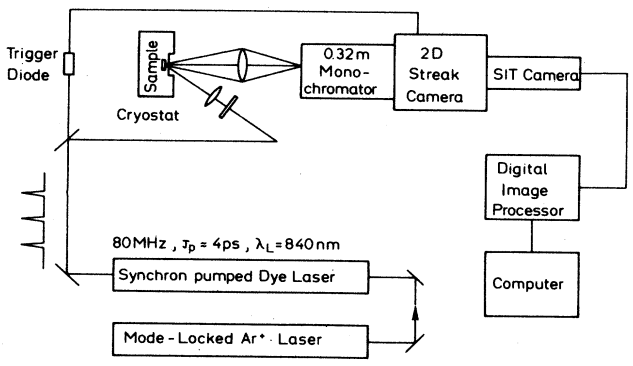

FIG. 1. Experimental setup for the time-resolved photoluminescence measurements. For explanations, see text.

III. BULK $Ga_{0.47}In_{0.53}As$

In Fig. 2 we show three transient photoluminescence spectra obtained from bulk $Ga_{0.47}In_{0.53}As$ at delay times of 40, 160, and 470 ps after the maximum of the excitation pulse for the highest excitation density of 2.2×10^{8} cm^{-3}. The photoluminescence is attributed mainly to radiative band-band recombination; on the low-energy side there might be a contribution of impurity-related recombination. Luminescence from excitonic transitions will not be considered, since excitons are damped out in bulk semiconductors at densities of a few 10^{15} cm^{-3} carriers/cm^3.[10]

We assume fast thermalization of electrons and holes as well as between electrons and holes via carrier-carrier collisions to analyze the experimental data. Inhomogeneous excitation and reabsorption are neglected. The luminescence spectra are fitted by a band-band recombination model assuming conservation of the wave vector k. This line fit shows a flat dependence of the luminescence intensity on photon energy between $h\nu=E_g$ and $h\nu=E_g+\mu_e$, where E_g is the band gap and μ_e is the quasi-Fermi-level for electrons, and an exponential decrease for $h\nu\geq E_g+\mu_e$. Therefore we obtain the density of excited carriers, which enters the line fit via the quasi-Fermi-levels of electrons, and the carrier temperature T_c, which determines the high-energy tail by the relation $I(h\nu)\propto\exp(-h\nu/kT_c)$. In that way the temperature of the carrier system is obtained as a function of excitation density and of delay time.

Figure 3 shows the temporal behavior of T_c for four excitation densities. A rapid cooling is observed in the first 100 ps for the highest excitation density of 2.2×10^{18} cm^{-3}, followed by a slower decrease of the carrier temperature at longer delay times. We have also measured T_c for dealy times as long as 1.5 ns and have observed a temperature of 40 K. Sample heating is therefore limited to temperatures below 40 K and the high temperature of 120 K after a 500-ps delay has a different physical origin. The cooling curves for lower initial excitation densities show, in principle, the same behavior, however, the initial cooling starts from a lower temperature and is faster. In addition, the carrier temperature after 500 ps is closer to the lattice temperature of 5 K.

The next step is the development of a theoretical model for carrier cooling, which allows one to extract the strength of the different energy-loss and heating mechanisms from the cooling data. We use Fermi-Dirac statistics for electrons and holes, because for excitation densities in the range of 10^{18} cm^{-3} the electronic system is highly degenerate. The most important energy-loss mechanism for carrier temperatures above 40 K is polar-optical scattering. The polar-optical ELR per electron for a degenerate distribution is given by[11]

$$\left[\frac{dE}{dt}\right]_{PO}=P_0x_c^{1/2}\frac{2}{\sqrt{\pi}}\frac{1}{F_{1/2}(\eta)}\left[N_q\int_0^\infty f(\varepsilon)[1-f(\varepsilon+x_c)]\sinh^{-1}\left[\frac{\varepsilon}{x_c}\right]^{1/2}d\varepsilon\right.$$
$$\left.-(N_q+1)\int_0^\infty f(\varepsilon+x_c)[1-f(\varepsilon)]\sinh^{-1}\left[\frac{\varepsilon}{x_c}\right]^{1/2}d\varepsilon\right], \quad (1)$$

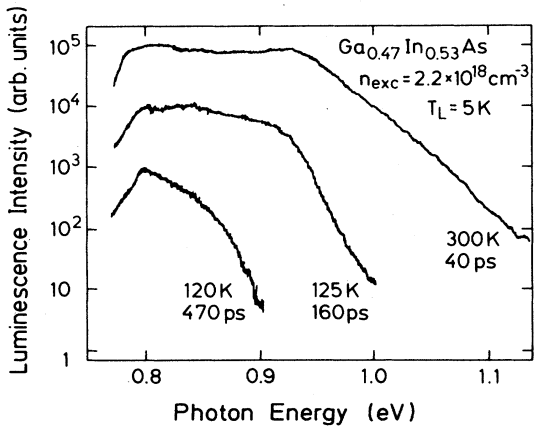

FIG. 2. Transient photoluminescence spectra for bulk $Ga_{0.47}In_{0.53}As$ at three different delay times (40, 160, and 470 ps) depicted for an excitation density of 2.2×10^{18} cm^{-3}. The spectra have been normalized to the respective maximum and multiplied by a factor of 10^5, 10^4, and 10^3 for delay times of 40, 160, and 470 ps, respectively.

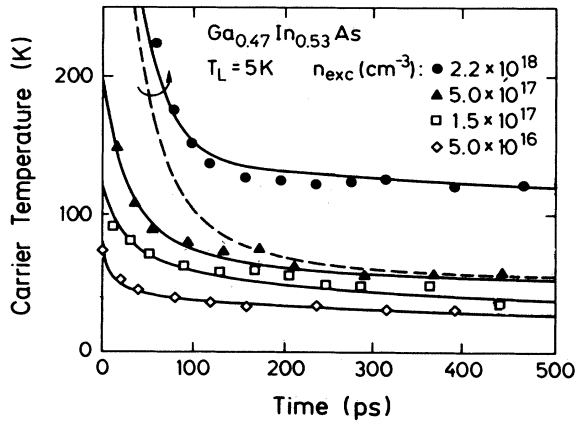

FIG. 3. Cooling data of bulk $Ga_{0.47}In_{0.53}As$ for different excitation densities. Theoretical fits calculated by the model of carrier cooling explained later in the text are depicted (solid curves) using $E_{ac}=3$ eV and $F=100$, 70, 40, and 3 for excitation densities of 2.2×10^{18}, 5×10^{17}, 1.5×10^{17}, and 5×10^{16} cm^{-3}. The dashed line shows a theoretical curve for the highest excitation density calculated with the same parameters as the corresponding solid line, but neglecting Auger recombination.

where $P_0=\hbar\omega_{LO}/\tau_e$, $\hbar\omega_{LO}$ is the energy of the longitudinal-optical phonon, $\tau_e=0.16$ ps is the electron–LO-phonon scattering time, $x_c=\hbar\omega_{LO}/kT_c$, $N_q=1/(e^{x_0}-1)$ is the occupation number for LO phonons with $x_0=\hbar\omega_{LO}/kT_L$, where T_L is the lattice temperature, $f(\varepsilon)=1/[1+\exp(\varepsilon-\eta)]$ is the occupation probability for electrons with $\varepsilon=E/kT_c$ and $\eta=E_F/kT_c$, and

$$F_j(\eta)=\frac{1}{\Gamma(j+1)}\int_0^\infty \frac{\varepsilon^j d\varepsilon}{1+\exp(\varepsilon-\eta)} \tag{2}$$

is the Fermi integral of index j. The material parameters entering in this and the following equations are listed in Table II.

Equation (1) is valid only for electrons and consists of two parts, the first describing the absorption and the second the emission of LO phonons by electrons. The polar-optical ELR for heavy holes is obtained by using the effective mass of heavy holes instead that of electrons. In addition, the rate must be reduced by a factor of 2, because the theory of polar-optical scattering is calculated with s-like wave functions, whereas holes are described by wave functions with p-like symmetry.[13] These wave functions produce a smaller overlap in the matrix element of the Fröhlich Hamiltonian, which must be compensated. Concerning the light holes we note that the occupation probability is proportional to m^*_{LH}/m^*_{HH}. There are much fewer light holes than heavy holes because of the small effective mass and these fewer light holes scatter less efficiently with LO phonons than heavy holes. It is therefore justified to neglect energy loss by light holes in the theoretical model.

Holes also lose energy to the transverse- optical (TO-) phonon system via the nonpolar-optical deformation potential. Since this energy-loss rate has a similar analytical dependence on carrier energy, density, and temperature as polar-optical scattering, we subsum nonpolar-optical scattering under the polar-optical energy loss. This procedure seems reasonable, since we determine the strength of the polar energy loss by a fitting procedure. We use a factor F to reduce the theoretical polar-optical energy-loss rate,

$$\left[\frac{dE}{dt}\right]_{PO,expt}=\frac{1}{F}\left[\frac{dE}{dt}\right]_{PO,theor}. \tag{3}$$

This reduction factor F phenomenologically describes the reduction of the polar-optical energy loss because of screening of the Coulomb interaction between a single carrier and the lattice as well as other carriers and because of the buildup of a nonthermal distribution of LO phonons (LO-phonon bottleneck). Screening weakens the interaction and thereby reduces the emission of LO phonons. In the presence of nonthermal LO-phonon distribution the occupation number for LO phonons is much larger than the equilibrium value of Eq. (1). In that case the probability for the absorption of a LO phonon becames comparable with that of an emission of a LO phonon. Therefore the net polar-optical ELR will be strongly reduced.

The next important energy-loss mechanism, especially for carrier temperatures $T_c\leq 40$ K, is acoustic deformation-potential scattering, which is generally explained in the framework of crystal deformations. The ELR by this scattering mechanism is given by[11]

$$\left[\frac{dE}{dt}\right]_{DP}=-\frac{8\sqrt{2}}{\pi^{3/2}}\frac{(m^*)^{5/2}E_1^2}{\rho\hbar^4}(kT_c)^{3/2}\times\left[1-\frac{T_L}{T_c}\right]\frac{F_1(\eta)}{F_{1/2}(\eta)}, \tag{4}$$

where E_1 is the acoustic deformation potential for electrons and ρ is the density of mass of $Ga_{0.47}In_{0.53}As$. The ELR by acoustic deformation-potential scattering of holes is obtained using the effective mass of heavy holes and an acoustic deformation potential E_{ac} for holes. Because of the $(m^*)^{5/2}$ dependence the energy loss by acoustic deformation-potential scattering of holes by far exceeds that of electrons.

Piezoelectric scattering must be only considered for $T_c\leq 20$ K. It can therefore be neglected in our calculations, since we are interested in the temperature range above 20 K.

In addition, carrier heating by Auger processes has to be taken into account in narrow-gap materials. The heating rate per electron or hole is proportional to $C_{CHCC}npE_g$ for the conduction-band Auger process and to $C_{CHSH}npE_g$ for the valence-band Auger process (n and p are the concentrations of electrons and holes; C_{CHCC} and C_{CHSH} are the Auger coefficients for the respective Auger processes). In undoped samples we cannot distinguish the contributions of the different Auger processes ($n=p$) and therefore the heating rate simplifies to $C_An^2E_g$ with $C_A=C_{CHCC}+C_{CHSH}$. In GaAs Auger heating can be neglected because of the much smaller Auger coefficients.

We use Fermi-Dirac statistics for electrons and holes to model the cooling dynamics of the carrier system. Thus effects of recombination heating[14] are included. For the lifetime of the carriers we use the value for the lowest excitation density (2.6 ns for the bulk sample), which can

TABLE II. Parameters for $Ga_{0.47}In_{0.53}As$ from Ref. 12.

Electron effective mass	m_e^*	$0.041m_0$
Hole effective mass	m_h	$0.5m_0$
Static dielectric constant	ε_0	13.73
High-frequency dielectric constant	ε_∞	11.36
Acoustic deformation potential for electrons	E_1	5.9 eV
Density of mass of $Ga_{0.47}In_{0.53}As$	ρ	5.89 g/cm^{-3}
Electron–LO-phonon scattering time	τ_{e0}	0.16 ps
Hole–LO-phonon scattering time	τ_{h0}	0.09 ps

be determined from the temporal decay of the wavelength-integrated luminescence. For higher excitation density the carrier lifetime decreases mainly because of the increasing importance of Auger processes, but the evaluation via the wavelength-integrated luminsence becomes much more difficult.

We can now perform theoretical calculations of the cooling behavior of an electron hole plasma, taking into account the described energy-loss and heating mechanisms. The acoustic deformation potential E_{ac} for holes, the Auger coefficient C_A, and the reduction factor F of the polar-optical energy loss are treated as free parameters. We assume the Auger coefficient and the acoustic deformation potential of holes to be independent of excitation density, but allow a variation of the polar-optical ELR with excitation density. This assumption seems reasonable, because in the case of the Auger processes the dependence on carrier density is explicitly expressed. Theoretical work, in which screening of the acoustic deformation potential in 3D systems is postulated,[15] is not yet verified. In addition, we will show in this publication that even the long-range Fröhlich interaction, which causes polar-optical scattering, does not screen for holes in 2D systems. We assume therefore that also the short-range acoustic deformation potential will not be influenced dramatically by effects of screening.

The *a priori* unknown parameters, the reduction factor F of the polar-optical energy loss, the acoustic deformation potential of holes, E_{ac}, and the Auger coefficient C_A are determined nearly independently. The rapidly decreasing parts of the cooling curves at times less than 100 ps after the excitation are caused by polar-optical scattering and can therefore be used to determine the value of the polar-optical ELR according to Eq. (3). Acoustic deformation-potential scattering of holes is the dominant cooling process for low excitation densities and $T_c \leq 40$ K. Therefore a suitable fit of the cooling curve at the lowest excitation density of 5×10^{16} cm^{-3} yields the acoustic deformation-potential constant E_{ac} for holes in bulk $Ga_{0.47}In_{0.53}As$. Heating by Auger processes plays the most important role at the highest excitation density. We attribute the relatively high nonequilibrium carrier temperature of over 100 K for times longer than 100 ps to heating by Auger processes, and therefore deduce the value for the Auger coefficient from this part of the cooling curve at highest excitation. We obtain the solid lines in Fig. 3, which represent fits of the cooling of the electron-hole plasma calculated by our theoretical model. We will first discuss the intensity dependence of the polar-optical ELR. A factor of $F=3$ is obtained for the lowest excitation density of 5×10^{16} cm^{-3} by fitting the theoretical model to the experimental data. This factor is close to the value found in cw photoluminescence experiments[4] and the theoretical 3D value. For higher excitation densities of 1.5×10^{17}, 5×10^{17}, and 2.2×10^{18} cm^{-3}, we need reduction factors of 40, 70, and 100. As a result, a polar-optical ELR is obtained that is close to the theoretical expectation at low excitation density, but is strongly reduced with increasing excitation density. This observation is in contrast to the work of Kash and Shah.[2] An interpretation for this strong reduction of the polar-optical ELR will be given in Sec. VI of this paper.

A value of $E_{ac}=3$ eV gives a good fit to the cooling curve at lowest excitation density. This value is approximately half of the acoustic deformation potential of $E_1=5.9$ eV of electrons.[12] A similar relation between E_{ac} and E_1 has been also obtained for GaAs.[13]

Finally, an Auger coefficient of $C_A=7\times10^{-29}$ cm^{6}s^{-1} is necessary to approximate the cooling behavior at the highest excitation density. This value is in good agreement with other measurements of Auger coefficients in $Ga_{0.47}In_{0.53}As$ or materials with a comparable band gap.[16,17] We point out the importance of including carrier heating by Auger effects by depicting the dashed curve in Fig. 3. This curve is calculated with the same parameters as the solid curve for the highest excitation density, but neglecting Auger processes.

IV. UNDOPED MQW's

We next investigate whether the ELR's change at the transition from 3D to 2D or quasi-2D systems and whether these rates show a well-thickness dependence in MQW's. A systematic study of carrier cooling in undoped MQW's of different well thickness is performed using well thicknesses of 3.4, 8.0, and 13.8 nm (samples B, C, and D). The thin MQW B has only one confined electronic subband, whereas samples C and D have, respectively, three and four electronic subbands. In the experiment carriers are simultaneously excited into all states because of the applied excitation wavelength. The excitation density is varied again using neutral density filters and/or changing the size of the laser focus. Transient luminescence spectra at typical delay times are depicted in Fig. 4 for the different samples. These transient spectra indicate several complications in comparison to the luminescence spectra of the bulk sample.

First, in the thicker quantum wells of 8.0 and 13.8 nm well width part of the carriers are excited by the laser pulse to higher subbands and thus can change the cooling process. The energy position of the transitions corresponding to these higher subbands is marked by arrows in Figs. 4(b) and 4(c). The fundamental question is now whether we can assume a thermal equilibrium between the carriers and, in particular, the electrons in higher subbands and in the ground state. Recently, we investigated intersubband relaxation in an *n*-type modulation-doped $Ga_{0.47}In_{0.53}As/Al_{0.48}In_{0.52}As$ MQW and have found that the intersubband relaxation time should have a value between 0.5 (Ref. 18) and 3 ps (Ref. 19). Now an intersubband transition of electrons occurs mainly by scattering on a LO phonon; therefore intersubband relaxation times of *n*-type modulation-doped and undoped MQW's should be comparable. We can therefore assume that electrons and, more generally, carriers in different subbands are thermalized and can be described by a single distribution functions, at least for our time scales.

Second, excitons are much more important in two-dimensional structures than in bulk material, because the binding energy of 2D excitons is 4 times that of 3D excitons, and screening of the Coulomb interaction is much less effective in 2D than in 3D systems. In order to clari-

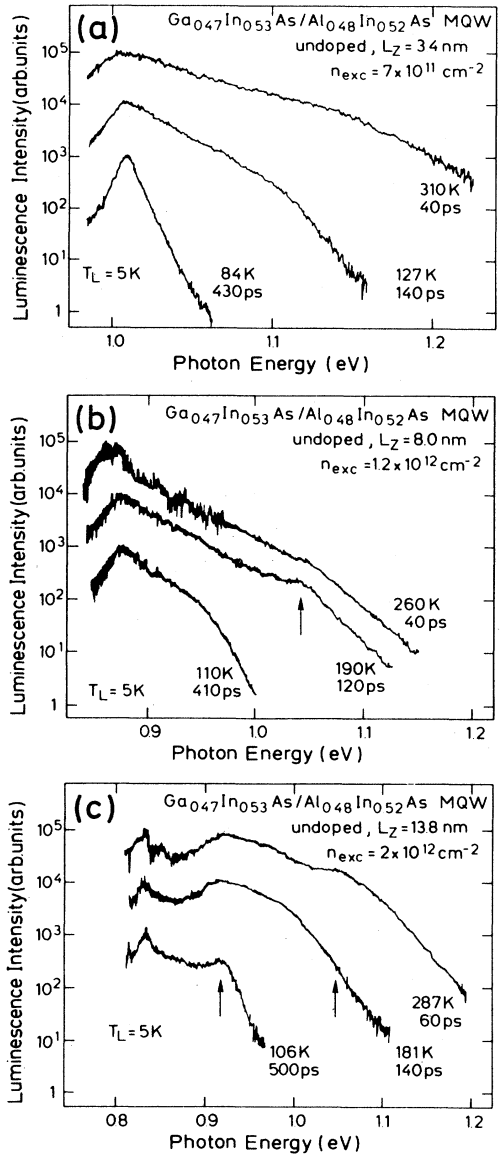

FIG. 4. Transient photoluminescence at different delay times of the MQW's with well thicknesses of (a) 3.4 nm, (b) 8.0 nm and (c) 13.8 nm in a plot corresponding to Fig. 2.

fy this point, we have studied the saturation of the excitonic resonance by free carriers in the 3.4-nm-thick MQW.[20] A value of 3.5×10^{10} cm^{-2} for the saturation density N_s is obtained in these experiments. We can thus neglect excitons for excitation densities, at which Fermi-Dirac statistics must be used. At lower excitation densities excitons are indeed present, but on the high-energy tail of the photoluminescence we always detect the temperature of free carriers.

Third, the part of the luminescence spectrum between the energy of the $n=1$ transition and the quasi-Fermi-level for electrons is not flat as expected from fits using band-band recombination with an energy-independent matrix element, but decreases towards higher photon energies, thus indicating an energy dependence of the matrix element of radiative recombination. The real problem is, however, that this dependence on photon energy seems to be a function of carrier temperature or density, as observed in Fig. 4(a) for the thinnest MQW.

Finally, the long carrier lifetime of 2.4 and 3 ns in the case of the 8.0- and 13.8-nm-thick MQW's results in an accumulation of carriers by successive laser pulses, which have a temporal spacing of 12.5 ns. The 2D picture of luminescence shows that the structures near the energy of the $n=1$ transition stem from a carrier-accumulation process and are therefore experimental artifacts. Carrier cooling as observed by the high-energy tails of the luminescence spectra, however, is not influenced by the accumulation process.

Considering these problems associated with luminescence spectra of 2D systems, we abstain from fitting the whole luminescence spectrum by a band-band recombination model and instead only extract the carrier temperature as a function of temporal delay with respect to the excitation pulse from the high-energy slope. The initial carrier density is estimated by measuring the size of the focal spot, the laser-pulse energy, and the absorption coefficient at the laser wavelength. The cooling curves derived in this manner are depicted in Fig. 5 for the different samples at various excitation densities.

Most of the theoretical work on scattering rates in 3D and 2D systems agrees that these rates are the same within a factor of about 2.[21,22] Since a careful analysis of such small-dimensional effects is beyond the scope of this paper, we use the outlined 3D formalism for analyzing the cooling behavior in 2D systems.

We discuss again the behavior of the polar optical ELR as a function of excitation density. Figure 6 shows the observed reduction factor F for the three MQW samples. The same strong reduction of the polar-optical ELR is found for increasing excitation density as in the bulk sample. A detailed discussion of the underlying mechanisms of this reduction will be given in Sec. VI. At this moment we will focus on three points.

First, in all three MQW samples the polar-optical ELR at low excitation density is comparable to theoretical (3D) expectations. Since the theoretically anticipated 2D scattering rates should be similar to the corresponding 3D ones, we conclude that the strength of the Fröhlich coupling in two dimensions is close to theoretical expectations. In addition, Fig. 6 shows a tendency of increasing coupling strength with decreasing well width, which is predicted also theoretically.[22]

Second, the Fröhlich coupling in 2D and 3D $Ga_{0.47}In_{0.53}As$ is comparable.

Third, we note that the reduction of the polar-optical ELR as a function of the sheet density n_2 as depicted in Fig. 6 is similar in all three samples. The possible mechanisms, which cause this reduction, namely LO-phonon overpopulation, screening of Coulomb interaction, or plasmon-phonon coupling should depend strongly on the sheet density in 2D or quasi-2D systems[23,24] and therefore the observed similar dependence of the polar-optical ELR on n_2 in all three MQW's is theoretically expected.

Next, we study the well-thickness dependence of the

ELR by acoustic deformation-potential scattering of holes. The strength of the acoustic deformation-potential scattering is proportional to $(m^*)^{5/2}E_{ac}^2$. For the bulk sample we know the effective mass of heavy holes and can therefore determine E_{ac} to 3 eV. In MQW's the effective mass of heavy holes as well as the acoustic deformation potential can show a dependence on well width and at present it is impossible to separate both effects. Figure 7 (solid dots, left-hand scale) shows the ELR by acoustic deformation-potential scattering of holes as a function of well thickness, normalized to the bulk value. A

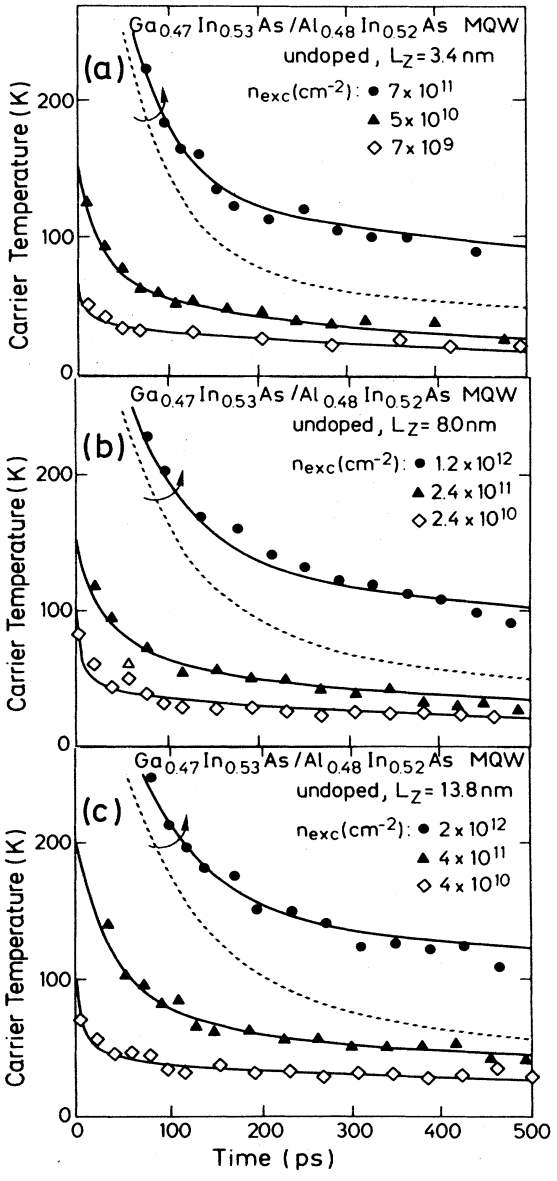

FIG. 5. Cooling curves for the MQW's with well thicknesses of (a) 3.4 nm, (b) 8.0 nm, and (c) 12.8 nm at different excitation densities. Theoretical fits (solid curves) use the reduction factors F of Fig. 6 and the deformation potential for holes and the Auger coefficients of Fig. 7.

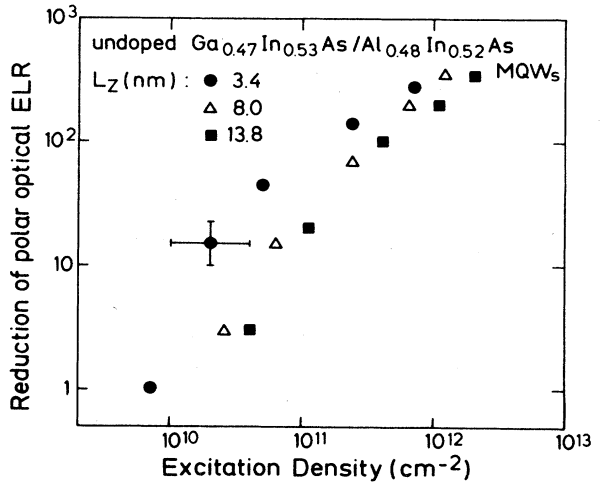

FIG. 6. The reduction of polar-optical ELR as a function of (two-dimensional) excitation density for the 3.4-nm MQW (circles), 8.0-nm MQW (triangles), and 13.8-nm MQW (squares).

significant increase is observed with decreasing well thickness. Further experiments are necessary to investigate the origin of this increase.

We discuss finally the well-thickness dependence of the Auger coefficients, which is also plotted in Fig. 7 (open squares, right-hand scale). A decreasing Auger coefficient with decreasing well thickness is observed (from 7×10^{-29} cm^{6}s^{-1} at a well thickness of 13.8 nm to 4×10^{-29} cm^{6}s^{-1} for 3.4 nm). This well-thickness dependence is explained by the normal dependence of the Auger effect on the size of the energy gap, which is observed also in the $Ga_xIn_{1-x}As_{1-y}P_y$ system.[17] We note that the Auger coefficients in the samples under investigation compare well with results obtained by a pump-and- probe technique in the same material[16] and in $Ga_xIn_{1-x}As_{1-y}P_y$ with a comparable band gap. There is no experimental evidence for a lower Auger coefficient in 2D structures in comparison to bulk material with a comparable band gap.

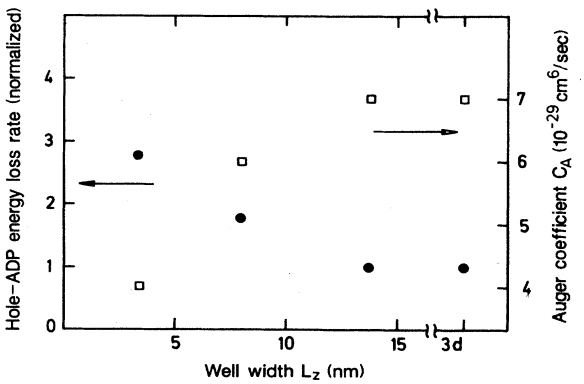

FIG. 7. The strength of acoustic deformation-potential scattering of holes (normalized to the bulk value) and the Auger coefficients as a function of well thickness.

V. MODULATION-DOPED MQS's

So far we have discussed the results obtained from undoped materials. Because of the excitation of electron-hole pairs, we can neither isolate the cooling behavior of one type of carriers nor attribute the observed reduction of the polar-optical ELR to a specific carrier type. A more detailed investigation of this phenomenon is possible in n- and p-type modulation-doped MQW's. The parameters of the samples E, F, and G are listed in Table I. The same luminescence experiment as described in Sec. II is performed with these samples. Transient luminescence spectra are shown in Fig. 8 for the two n-type and the p-type modulation-doped samples. The problems associated with higher subbands, energy-dependent matrix elements, and experimental artifacts are comparable to the case of undoped samples and will not be discussed. Carrier temperatures are derived from the high-energy tails of the transient luminescence spectra, leading to cooling curves, which are depicted in Fig. 9. The strength of the polar optical scattering, the acoustic deformation potential E_{ac} of holes, and the Auger coefficient are again determined by the described fitting procedure, taking into

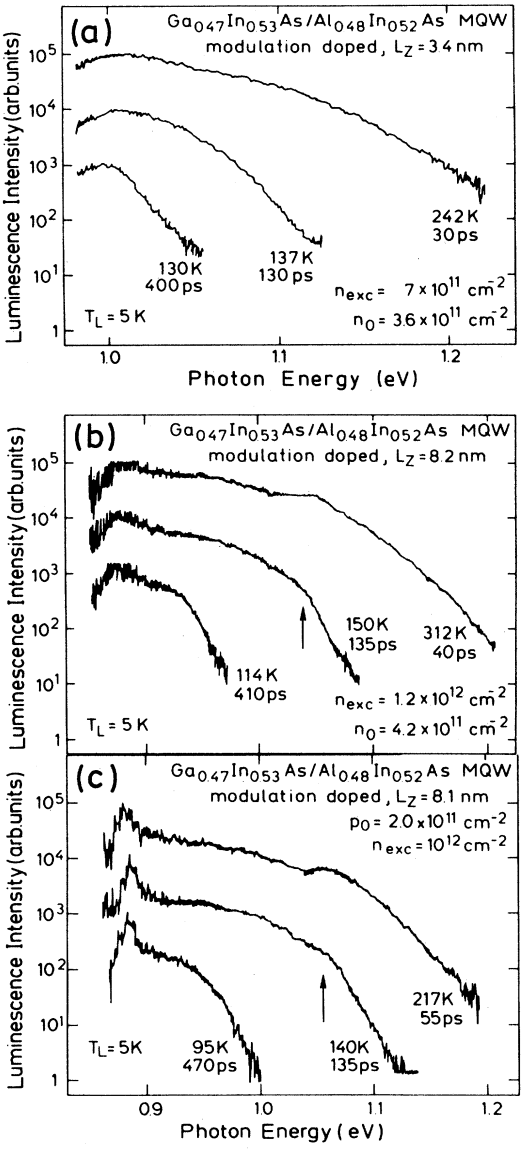

FIG. 8. Transient photoluminescence spectra for the modulation-doped MQW's. (a) and (b) show data for the 3.4- and 8.2-nm-thick n-type modulation-doped MQW's, whereas (c) shows spectra for the p-type modulation-doped sample in a plot corresponding to Fig. 2.

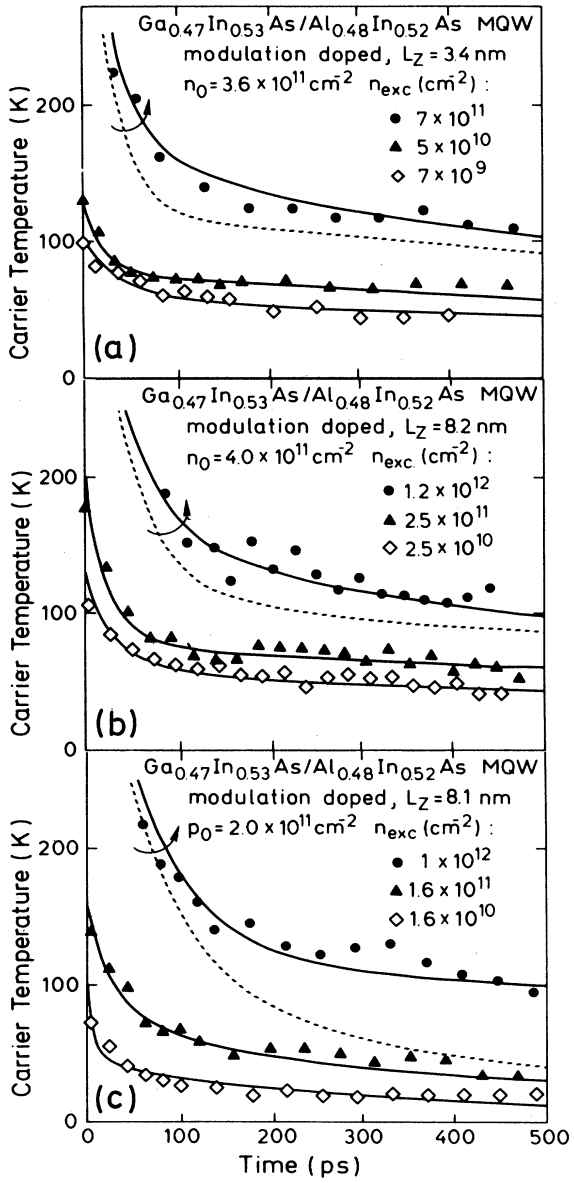

FIG. 9. Cooling curves for the modulation-doped MQW's at different excitation densities. (a) and (b) show the cooling behavior for the n-type modulation-doped samples, whereas (c) shows the p-type sample.

account the doping density of the respective sample. Before discussing the polar-optical energy-loss rates, a few additional points should be mentioned.

First, the carrier temperature of the *n*-type modulation-doped samples remains high for longer delay times even at moderate excitation densities. This behavior is explained by the strongly reduced importance of acoustic deformation-potential scattering of holes. The strength of acoustic deformation-potential scattering must be determined at excitation densities comparable to the doping density. In this case we find the same value as in comparable undoped specimens.

Second, the acoustic deformation potential observed in the *p*-type modulation-doped sample is the same as in undoped material. This result shows that acoustic deformation-potential scattering of holes will not be influenced noticeably by effects of screening at least up to a density of holes of 2×10^{11} cm^{-2}. This result justifies the unscreened acoustic deformation potential used in our model calculations.

Third, *CHCC* and *CHSH* Auger processes are not longer equivalent in modulation-doped samples. Nevertheless, at excitation densities, which are high in comparison to the doping density, both Auger processes became, in fact, unseparable again. We therefore use the same heating term as developed in Sec. III and find the same value for the Auger coefficients as for comparable undoped samples.

The reduction of the polar-optical ELR as a function of excitation density is plotted in Fig. 10. It is important to point out that the plot of the reduction of the polar-optical ELR against excitation density is a bit misleading, since the total carrier density is nearly constant in the case of weak excitation, but proportional to the excitation density for high excitation. The dependence of the energy-loss rates by electron–LO-phonon and hole–LO phonon scattering on excitation density (and also on total carrier density) is completely different. The polar-optical ELR of holes starts at approximately the theoretical value for low excitation density. For higher excitation densities we observe a reduction of the polar-optical ELR comparable to that in undoped samples. For the *n*-type modulation-doped samples, which have the same doping density and show an identical behavior, we see a reduction of the polar-optical ELR rate by a factor of 35 even at the lowest excitation densities used in this experiment. This result is in excellent agreement with infrared pump-and-probe experiments on the 8.2-nm-thick MQW (sample F) (Ref. 19) and compares well with results on *n*-type modulation-doped GaAs MQW's obtained by Shah *et al.*[25] by means of cw photoluminescence experiments. For higher excitation density the polar-optical energy loss is further reduced.

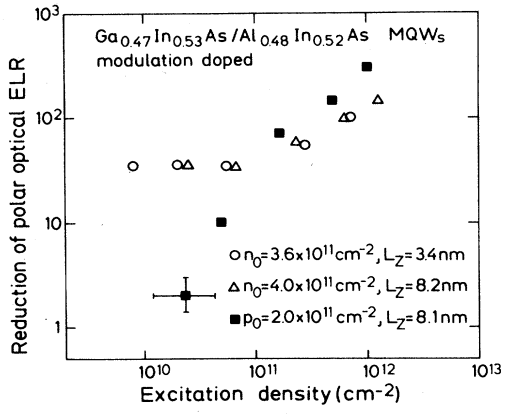

FIG. 10. Reduction of polar-optical energy loss as a function of excitation density. Circles and triangles show data for the *n*-type modulation-doped samples, whereas squares give the reduction factor for the *p*-type modulation-doped sample.

VI. DISCUSSION

In this section of the paper we first discuss the behavior of the polar-optical ELR in bulk $G_{0.47}In_{0.53}As$ and in undoped and modulation-doped $Ga_{0.47}In_{0.53}As/Al_{0.48}In_{0.52}As$ MQW's as a function of excitation density, and second we compare our results with earlier publications. The key feature for a qualitative understanding of the mechanisms, which cause the strong dependence of the polar-optical ELR on excitation density, is given by the results of the *p*-type modulation-doped MQW (see Fig. 10). We observe a strong reduction of the polar-optical ELR for excitation densities considerably below the doping density; that is, at nearly constant total carrier density. Screening of the Coulomb interaction as well as plasmon-phonon coupling depends sensitively on the total density of carriers.[13,36] We therefore conclude that these mechanisms are ruled out for the explanation of the observed strong reduction of the polar-optical ELR in the *p*-type modulation-doped MQW by experimental findings, and assume that the discussed reduction is caused by the remaining mechanism, an overpopulation of those LO-phonon modes, which are involved in the cooling process of holes. This LO-phonon overpopulation has been proposed by Pötz and Kocevar.[27] These authors have shown theoretically that the polar-optical ELR is substantially reduced by the existence of such a LO-phonon bottleneck. Screening and plasmon-phonon coupling might play a certain role for excitation densities higher than the doping density.

A comparison of the influence of hot LO phonons on electrons and holes implies that a significantly greater effect is expected for electrons, since the k space of LO phonons, which interact with the respective carrier type, scales in a simple parabolic band approximation as $(m^*)^{\nu/2}$, ν being the dimension of the carrier system. In addition, electrons will be screened by holes in undoped samples. We therefore expect that the polar-optical ELR of electrons is reduced at significantly lower excitation densities than that of holes. For this reason the dependence of the polar-optical ELR on excitation density in undoped samples will be determined by the excitation-density dependence of the polar-optical ELR of holes.

This expectation is confirmed when we compare the reduction of the polar-optical ELR in modulation-doped sample with the corresponding reduction in the undoped sample. Essentially the same behavior is observed in both samples. Therefore the observed reduction of the polar-optical ELR at high excitation densities in undoped 2D and 3D samples should be mainly caused by a nonthermal population of LO phonons, which are involved in the cooling process of holes.

The dynamics of the polar-optical ELR of electrons can only be studied in *n*-type modulation-doped MQW samples. The interesting new feature is the leveling of the reduction factor as observed in Fig. 10 for low excitation densities. As explained earlier, electrons are more sensitive to LO-phonon overpopulation than holes. Comparing now the excitation dependence of polar-optical energy loss of the *n* and *p*-type samples, we certainly have experimental conditions in which an overpopulation of LO phonons, which are involved in the cooling of electrons, can reduce the polar-optical energy loss of electrons. However, even among theoreticians there exists a considerable disagreement about the influence of screening on the polar-optical ELR of electrons. Yoffa[28] claims that in 3D GaAs the polar-optical energy-loss rate of electrons should decrease at densities as low as 6×10^{16} cm^{-3}, whereas Das Sarma *et al.*[29] give a value of 5×10^{17} cm^{-3}. Of course, we cannot straightforwardly compare GaAs and $Ga_{0.47}In_{0.53}As$ as well as 3D and 2D material. Nevertheless, the cited papers show that at the carrier densities used here as doping densities screening might reduce also the polar-optical ELR of hot electrons. The problem is that screening and a hot phonon effect compete with each other, i.e., the existence of screening reduces the phonon overpopulation. We therefore conclude that a separation of effects due to screening and to LO-phonon overpopulation is not possible with this type of experiment in *n*-type modulation-doped MQW's. In our opinion the main effect is caused by a LO-phonon overpopulation, but screening might play an additional role.

We now compare the results reported in this paper with results published by other groups. The first measurements on carrier cooling in $Ga_{0.47}In_{0.53}As$ were reported by Kash and Shah,[2] using a 0.5-μm-thick epilayer of $Ga_{0.47}In_{0.53}As$. A strongly reduced polar-optical ELR independent on excitation density has been observed for excitation densities of 7×10^{17} and 2×10^{18} cm^{-3}. In that paper Maxwell-Boltzmann statistics has been used for analyzing the cooling data and only energy loss by polar-optical scattering has been taken into account. In addition, the range of excitation densities has been too small to make definitive claims about the dependence of the polar-optical energy loss on excitation density, especially for low carrier densities. If we neglect discrepancies in the numerical value of the reduction of the polar-optical ELR, which are caused by our more accurate theoretical model, these earlier measurements can be regarded as the high excitation limit of the measurements reported in Sec. III.

The results of Shum *et al.*,[3] which claim a reduction of polar-optical energy loss by a factor of 300 in a cw experiment at excitation densities of 10^{15} cm^{-3} in $Ga_{0.47}In_{0.53}As/Al_{0.48}In_{0.52}As$ single quantum wells, are in strong contradiction to the results of our cw experiment[4] and to the time-resolved data presented in this paper, especially the dependence of polar-optical energy loss on excitation densities. The origin of this discrepancy is not clear. We suppose that the determination of the excitation density, which enters critically the calculation of the polar-optical energy loss in the work of Shum *et al.*, is rather uncertain because of the indirect excitation. Another problem are the trapping times used in the theoretical treatment of Ref. 3.

The strongly reduced polar-optical ELR in *n*-type modulation-doped MQW's was first reported by Ryan *et al.*[30] in the GaAs system. This reduction was attributed rather to a reduced Fröhlich coupling in 2D systems than to the doping density of electrons. However, in the work of Shah[25] and of ourselves[7] it has been shown that this reduction of polar-optical energy loss in *n*-type modulation-doped MQW's is caused by the doping density of electrons and has therefore nothing to do with the reduced dimensionality of the coupled carrier–LO-phonon system.

The result that the reduction of the polar-optical ELR behaves similarly in undoped MQW's of different well thickness, when it is plotted as a function of the 2D excitation density, has been reported recently in the GaAs system.[31–33] The claim, however, that this dependence indicates a hot LO-phonon effect[32] is not correct. All mechanisms which cause a reduction of the polar-optical ELR, i.e., screening of the Coulomb interaction, plasmon-phonon coupling, and a nonequilibrium LO-phonon population, should depend on the 2D excitation density n_2 in quasi-two-dimensional systems.

Finally, the observation that the polar-optical energy loss of holes is not influenced by effects of screening, at least up to densities of 2×10^{11} cm^{-2}, and that the observed reduction of this loss must therefore be caused by LO-phonon overpopulation, is confirmed by the experiments of Rühle *et al.*[34] and Polland *et al.*[35] The results of these papers show that the polar-optical ELR in undoped samples, which is determined by the polar-optical ELR of holes, is not influenced by the carrier density up to 3D excitation densities of 4×10^{17} cm^{-3} or 2D densities of 4×10^{11} cm^{-2}.

VII. CONCLUSIONS

We have studied the cooling of hot carriers in an undoped $Al_{0.48}In_{0.52}As/Ga_{0.47}In_{0.53}As/InP$ heterostructure and in undoped and modulation-doped $Ga_{0.47}In_{0.53}As/Al_{0.48}In_{0.52}As$ MQW's. The observed polar-optical ELR of holes is in good agreement with the theoretical value for low excitation densities, whereas it is reduced by 2 orders of magnitude at high excitation according to a hot phonon effect. For electrons the polar-optical energy-loss rate is strongly reduced, even at low excitation density. In explaining this reduction we cannot rule out a certain screening of the Coulomb interaction.

In addition, we find a well-thickness dependence of the acoustic deformation-potential scattering of holes and of the Auger processes. Acoustic deformation-potential scattering increases with decreasing well thickness due to an increase of the acoustic deformation potential of holes, E_{ac}, and/or of the effective mass of holes. The Auger processes become less important with decreasing well thickness, which represents the expected dependence on energy gaps.

ACKNOWLEDGMENTS

We thank H. J. Queisser and J. Kuhl for a critical reading of the manuscript and valuable discussions. The technical assistance of K. Rother is gratefully acknowledged. Part of this work was sponsored by the Stiftung Volkswagenwerk and by the Bundesministerium für Forschung and Technologie of the Federal Republic of Germany.

[1]J. Shah, IEEE J. Quantum Electron. **QE-22**, 1728 (1986).
[2]K. Kash and J. Shah, Appl. Phys. Lett. **45**, 401 (1984).
[3]K. Shum, P. P. Ho, R. R. Alfano, D. F. Welch, G. W. Wicks, and L. F. Eastman, IEEE J. Quantum Electron. **QE-22**, 1811 (1986).
[4]H. Lobentanzer, W. W. Rühle, W. Stolz, and K. Ploog, Solid State Commun. **62**, 53 (1987).
[5]H. Lobentanzer, H.-J. Polland, W. W. Rühle, W. Stolz, and K. Ploog, Appl. Phys. Lett. **51**, 673 (1987).
[6]H. Lobentanzer, H.-J. Polland, W. W. Rühle, W. Stolz, and K. Ploog, Phys. Rev. B **36**, 1136 (1987).
[7]H. Lobentanzer, W. W. Rühle, H.-J. Polland, W. Stolz, and K. Ploog, Phys. Rev. B **36**, 2954 (1987).
[8]W. Stolz, J. C. Maan, M. Altarelli, L. Tapfer, and K. Ploog, Phys. Rev. B **36**, 4301 (1987).
[9]W. Stolz, J. C. Maan, M. Altarelli, L. Tapfer, and K. Ploog, Phys. Rev. B **36**, 4310 (1987).
[10]E. O. Göbel and G. Mahler, in *Festkörperprobleme (Advances in Solid State Physics)*, edited by J. Treusch (Vieweg, Braunschweig, 1979), Vol. 19, pp. 109–158.
[11]J. Shah and R. F. Leheny, in *Semiconductors Probed by Ultrafast Laser Spectroscopy*, edited by R. R. Alfano (Academic, New York, 1984), pp. 45–73.
[12]Y. Takeda, in *GaInAsP Alloy Semiconductors*, edited by T. P. Pearsall (Wiley, New York, 1982), pp. 213–241.
[13]E. O. Göbel and O. Hildebrand, Phys. Status Solidi B **88**, 645 (1978).
[14]D. Bimberg and J. Mycielski, Phys. Rev. B **31**, 5490 (1985).
[15]M. Pugnet, J. Collet, and A. Cornet, Solid State Commun. **38**, 531 (1981).
[16]B. Sermage, D. S. Chemla, D. Sivco, and A. Y. Cho, IEEE J. Quantum Electron. **QE-22**, 774 (1986).
[17]E. Wintner and E. P. Ippen, Appl. Phys. Lett. **44**, 999 (1984).
[18]H. Lobentanzer, W. König, W. Stolz, K. Ploog, T. Elsaesser, and R. J. Bäuerle, Appl. Phys. Lett. **53**, 571 (1988).
[19]R. J. Bäuerle, T. Elsaesser, W. Kaiser, H. Lobentanzer, W. Stolz, and K. Ploog, Phys. Rev. B **38**, 4307 (1988).
[20]H. Lobentanzer, doctoral thesis, University of Stuttgart, 1988.
[21]P. J. Price, Ann. Phys. (N.Y.) **133**, 217 (1981).
[22]F. A. Riddoch and B. K. Ridley, J. Phys. C **16**, 6971 (1983).
[23]P. Lugli and S. M. Goodnick, Phys. Rev. Lett. **59**, 716 (1987).
[24]B. A. Mason and S. Das Sarma, Phys. Rev. B **35**, 3890 (1987).
[25]J. Shah, A. Pinczuk, A. C. Gossard, and W. Wiegmann, Phys. Rev. Lett. **54**, 2045 (1985).
[26]J. Collet, A. Cornet, M. Pugnet, and T. Amand, Solid State Commun. **42**, 883 (1982).
[27]W. Pötz and P. Kocevar, Phys. Rev. B **28**, 7040 (1983).
[28]E. Yoffa, Phys. Rev. B **23**, 1909 (1981).
[29]S. Das Sarma, J. K. Jain, and R. Jalabert, Phys. Rev. B **37**, 6290 (1988).
[30]J. F. Ryan, A. J. Turberfield, A. Maciel, J. M. Worlock, A. C. Gossard, and W. Wiegmann, Phys. Rev. Lett. **54**, 2045 (1985).
[31]K. Leo, W. W. Rühle, H. J. Queisser, and K. Ploog, Appl. Phys. A **45**, 35 (1988).
[32]K. Leo, W. W. Rühle and H. J. Queisser, and K. Ploog, Phys. Rev. B **37**, 7121 (1988).
[33]K. Leo, W. W. Rühle, and K. Ploog, Phys. Rev. B **38**, 1947 (1988).
[34]W. W. Rühle, and H.-J. Polland, Phys. Rev. B **36**, 1683 (1987).
[35]H.-J. Polland, W. W. Rühle, K. Ploog, and C. W. Tu, Phys. Rev. B **36**, 7722 (1987).